EPJ Web of Conferences **262**, 01014 (2022) https://doi.org/10.1051/epjconf/202226201014
EXA2021

BRAND – exploring transverse polarization of electrons emitted in neutron decay

Feasibility demonstration experiment

K. Bodek[1,*], *J.* Choi[5], *L.* De Keukeleere[3], *K.* Dhanmeher[2], *M.* Engler[6], *G.* Gupta[1], *A.* Kozela[2], *K.* Lojek[1], *K.* Pysz[2], *D.* Ries[6], *D.* Rozpedzik[1], *N.* Severijns[3], *T.* Soldner[4], *N.* Yazdandoost[6], *A.R.* Young[5], and *J.* Zejma[1]

[1]M. Smoluchowski Institute of Physics, Jagiellonian University, Krakow, Poland
[2]H. Niewodniczanski Institute of Nuclear Physics, Polish Academy of Sciences, Krakow, Poland
[3]Institute of Nuclear and Radiation Physics, KU Leuven, Belgium
[4]Institut Laue-Langevin, Grenoble, France
[5]Dep. of Physics and Astronomy, North Carolina State University, Raleigh, USA
[6]Dep. of Chemistry, TRIGA site, J. Gutenberg University, Mainz, Germany

Abstract. Neutron and nuclear beta decay correlation coefficients are sensitive to the exotic scalar and tensor interactions that are not included in the Standard Model (SM). The proposed experiment BRAND will measure simultaneously seven neutron correlation coefficients: H, L, N, R, S, U and V that depend on the transverse electron polarization – a quantity which vanishes in the SM. Five of these correlations: H, L, S, U and V were never attempted experimentally before. The expected impact of the proposed experiment is comparable to that of frequently measured "traditional" correlation coefficients (a, b, A, B, D) but offers completely different systematics and additional sensitivity to imaginary parts of the scalar and tensor couplings. In order to demonstrate the feasibility of the challenging techniques such as the event-by-event decay kinematics reconstruction together with the electron polarimetry a test setup was installed at the cold neutron beam line PF1B at the Laue-Langevin Institute, Grenoble, France. In this contribution, the results of the first run as well as plans for the run in Autumn 2021 will be discussed.

1 Introduction

Among the empirical foundations of the electroweak standard model (SM) the assumptions of maximal parity violation, vector and axial-vector character and massless neutrinos are directly linked to the experiments performed with the nuclear and neutron beta decay. The beta decay theory has been firmly established about six decades ago and became a part of the SM. Nevertheless, despite the great success of the SM, many open questions remain such as the origin of parity violation, the hierarchy of fermion masses, the number of particle generations, the mechanism of CP violation, the worrying large number of parameters of the theory, etc. Nuclear beta decay experiments test weakly interacting systems and free neutron

*e-mail: kazimierz.bodek@uj.edu.pl

decay plays a particular role: due to its simplicity it is free of complications connected with the nuclear and atomic structure.

The neutron beta decay is an allowed and mixed transition. Contrary to the nuclear mixed beta transitions, the Fermi and Gamow-Teller contributions to the neutron decay rate and energy-angle distribution are known accurately since the corresponding matrix elements are not affected by nuclear structure uncertainties. In the SM, the neutron beta decay is described by only two parameters: the V_{ud} element of the Cabibo-Kobayashi-Maskawa mixing matrix and the ratio of the axial vector to vector charges, $\lambda = g_A/g_V$. The large number of the experimental observables depending on the momenta and spins of the involved particles makes the situation highly redundant and attractive for precision experiments aiming at the improvement of the SM and searching for effects which cannot be explained by the SM. For instance, the SM predictions of time-reversal violation for weak decays of systems built up of u and d quarks are by 7 to 10 orders of magnitude lower than the experimental accuracies attainable at present. The exploration of this intriguing window is mitigated by the accuracy of theoretically calculated electromagnetic (EM) corrections which presently achieve the level slightly better than 10^{-4} [1, 2].

2 Transverse electron polarization in neutron decay

Generally, in the Standard Model, the electrons emitted in beta decay are longitudinally polarized which reflects the parity violating V-A structure of the weak interaction. The departure of the polarization vector from a strict collinearity with electron momentum can be caused by electromagnetic effects, recoil order corrections (induced couplings) or exotic scalar and tensor interactions. Thus, provided that the electromagnetic and recoil order corrections are under control, the transverse electron polarization is an ideal observable for searches of physics beyond the Standard Model.

The transverse electron polarization is reflected in the distribution of the decay products via a number of the correlation coefficients relating it to other vectors characterizing the system, the most important being the electron and antineutrino momenta $\mathbf{p}_e$, $\mathbf{p}_{\bar{\nu}}$ and the neutron spin $\mathbf{J}$. The corresponding formula limited to the lowest order terms can be found in the classical papers [3–5]. Dropping out all the terms not depending explicitly on the transverse components of the electron polarization and retaining five exceptions: a, b, A, B and D ("classical" correlations) one arrives at:

$$\begin{aligned}
&\omega(E_e, \Omega_e, \Omega_{\bar{\nu}}) \;\propto\; 1 + \\
&a\,\frac{\mathbf{p}_e\cdot\mathbf{p}_{\bar{\nu}}}{E_e E_{\bar{\nu}}} + b\,\frac{m_e}{E_e} + \frac{\langle\mathbf{J}\rangle}{J}\cdot\left[A\,\frac{\mathbf{p}_e}{E_e} + B\,\frac{\mathbf{p}_{\bar{\nu}}}{E_{\bar{\nu}}} + D\,\frac{\mathbf{p}_e\times\mathbf{p}_{\bar{\nu}}}{E_e E_{\bar{\nu}}}\right] + \\
&\boldsymbol{\sigma}_\perp\cdot\left[H\,\frac{\mathbf{p}_{\bar{\nu}}}{E_{\bar{\nu}}} + L\,\frac{\mathbf{p}_e\times\mathbf{p}_{\bar{\nu}}}{E_e E_{\bar{\nu}}} + N\,\frac{\langle\mathbf{J}\rangle}{J} + R\,\frac{\langle\mathbf{J}\rangle\times\mathbf{p}_e}{J\,E_e} + S\,\frac{\langle\mathbf{J}\rangle}{J}\,\frac{\mathbf{p}_e\cdot\mathbf{p}_{\bar{\nu}}}{E_e E_{\bar{\nu}}} + U\,\mathbf{p}_{\bar{\nu}}\frac{\langle\mathbf{J}\rangle\cdot\mathbf{p}_e}{J\,E_e E_{\bar{\nu}}} + V\,\frac{\mathbf{p}_{\bar{\nu}}\times\langle\mathbf{J}\rangle}{J\,E_{\bar{\nu}}}\right],
\end{aligned} \tag{1}$$

where $\boldsymbol{\sigma}_\perp$ represents a unit vector perpendicular to the electron momentum $\mathbf{p}_e$ and $J = |\mathbf{J}|$. In the infinite neutron mass approximation (no recoil), making usual assumptions for the Standard Model: $C_V = C'_V = 1$ and $\lambda \equiv C_A = C'_A = -1.272$ [6], and neglecting the contributions quadratic (and higher order) in C_S, C'_S, C_T, C'_T one can express all the correlation coefficients from Eq. (1) (called here X) as combinations of the real and imaginary parts of the scalar, $\mathfrak{S}$, and tensor, $\mathfrak{T}$, normalized exotic couplings:

$$X = X_{\mathrm{SM}} + X_{\mathrm{EM}} + c^X_{\mathrm{Re}S}\,\mathrm{Re}(\mathfrak{S}) + c^X_{\mathrm{Re}T}\,\mathrm{Re}(\mathfrak{T}) + c^X_{\mathrm{Im}S}\,\mathrm{Im}(\mathfrak{S}) + c^X_{\mathrm{Im}T}\,\mathrm{Im}(\mathfrak{T}) \tag{2}$$

with

$$\mathfrak{S} \equiv \frac{C_S + C'_S}{C_V}, \qquad \mathfrak{T} \equiv \frac{C_T + C'_T}{C_A}. \tag{3}$$

The coefficients c in this expression are functions of λ and kinematical quantities. Table 1 in Ref. [7] summarizes their values calculated with the kinematical factors averaged over the electron spectrum in the kinetic energy range 200–783 keV.

The coefficients relating the transverse electron polarization to $\mathbf{p}_e$, $\mathbf{p}_{\bar{\nu}}$ and $\mathbf{J}$ have several interesting features. They vanish for the SM weak interaction, reveal variable size of the EM contributions and are measurable using known techniques. And, last but not least, the dependence on real and imaginary parts of the scalar and tensor couplings alternates exclusively from one correlation coefficient to another with varying sensitivity coefficients.

3 BRAND project

The experiment reported in Refs. [9–12] has clearly proven that the transverse electron polarization of electrons emitted in the decay of cold neutrons can be accurately measured with Mott scattering. The applied technique of electron tracking and reconstruction of the scattering vertices is a powerful tool for reduction of background typical in experiments with intense neutron beams. The rich experience and quantitative information gained in that pioneering experiment allow for a realistic planning of the next steps.

The proposed experiment will measure the transverse electron polarization expressed in terms of 7 correlation coefficients (H, L, N, R, S, U, V) as compared to two (N, R) accessible in the former setup [9–12]. The simultaneous measurements of the coefficients a, A, B and D will help to keep systematics under control. It will be intriguing to compare their values with those from the specialized experiments [13–20] since our experimental technique is completely different.

The measurement of momenta of electrons and protons in coincidence will allow for reconstruction of the antineutrino momentum and will provide access to the terms dependent on this quantity. The strategy of the proposed experiment is to reconstruct event-by-event the decay kinematics and identify the decay origin. Such a condition will reduce the effects due to large size of the decay source, as well as scattering effects and will significantly suppress background. In particular, confining the three-body decay kinematics by the measured electron energy and relative $e - p$ angle one realizes that the proton energy and thus the proton time-of-flight must choose between two discrete (and known) values.

The key features of the proposed setup are: (i) Efficient cylindrical detector geometry. (ii) Electron tracking in a multi-wire drift chamber (MWDC) with hexagonal geometry of cells with signal readout at both wire ends operated in He/isobutane gas mixture. (iii) Detection of both direct and Mott-scattered electrons in plastic scintillator hodoscopes. (iv) Conversion of protons (accelerated to 20–30 keV) into bunches of secondary electrons ejected from a thin LiF layer [21]. Acceleration and subsequent detection of ejected electrons in a thin ($\sim$25 μm) plastic scintillator with position sensitivity. (v) Reduction of geometry misalignment related systematic effects by the use of advanced polarimetry techniques such as periodic neutron spin flip during data taking and evaluation of asymmetry and super-ratio in data analysis.

Background contributions will be subtracted using data collected in several regimes (beam-on, beam-off, Mott target-on, Mott target-off). In order to deduce necessary corrections and asses associated systematic errors, mapping of the spin guiding field and detector efficiency will be carried out in a series of calibration experiments.

A cross section of the proposed cylindrical Mott polarimeter for decay electrons and accompanying detectors for recoil protons is sketched in Figure 1. Decay electrons reach

the Mott target made a of 1–2 μm thick layer of high Z element (lead or depleted uranium) deposited on a thin Mylar substrate. The decay electrons can be either backscattered or pass the foil and be detected in the outer plastic scintillator hodoscope located close to it. The Mott-scattered electrons are registered in either of the inner hodoscopes as shown in Figure 1. The electron hodoscopes will be made of plastic scintillator bars readout by photomultiplier tubes attached to both bar ends. They will operate at ambient pressure outside of the vacuum chamber.

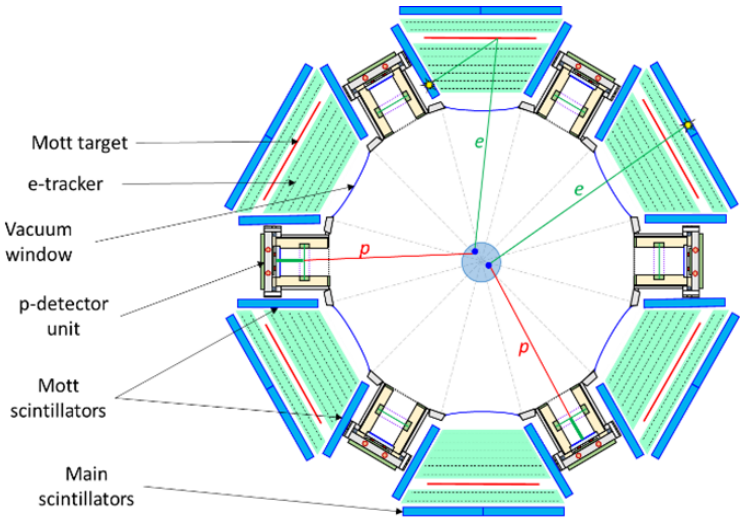

Figure 1. (Color on-line) Sketch of the proposed experimental setup in the cylindrical geometry.

After leaving the free drift zone, protons are accelerated by electric field towards a $p - e$ conversion foil consisting of a 20 nm thick LiF layer deposited onto a thin (100 nm) fluorinated-polyamide film [21]. The located in vacuum "proton" detectors will register bunches of up to 20 secondary electrons ejected from that foil. Acceleration and subsequent detection of ejected electrons is implemented using a thin ($\approx$25 μm) plastic scintillator film deposited onto light guides. The scintillation light will be registered by SiPM sensors attached along the light guide. The hit position information will be deduced from the distribution of the light signal registered by SiPM sensors close to the light flash source. The "proton" detector will be able to discriminate electrons from beta decay with energy higher than 30 keV since they deposit in it less than 30 keV while the accumulated signal from the electron bunch following the $p - e$ conversion corresponds to 100–500 keV.

3.1 Demonstration apparatus

The proposed BRAND experiment assumes several difficult techniques to be applied simultaneously. Among them are large area thin vacuum windows, precision low-mass, low-Z electron tracker and large acceptance recoil proton detector made of low Z materials (required to minimize backscattering of charged particles). In order to check the proposed solutions, in September 2020, a short test measurement (5 days) with the use of prototype BRAND apparatus (called BRAND-0 setup) was performed at the neutron facility PF1B of the Laue-Langevin Institute (ILL), Grenoble. Polarized cold neutron beam with a flux of 6.3×10^8

n/cm^2/s and cross-section of 6×6 cm^2 was used for this purpose. Fig. 2 shows a sketch of the BRAND-0 setup.

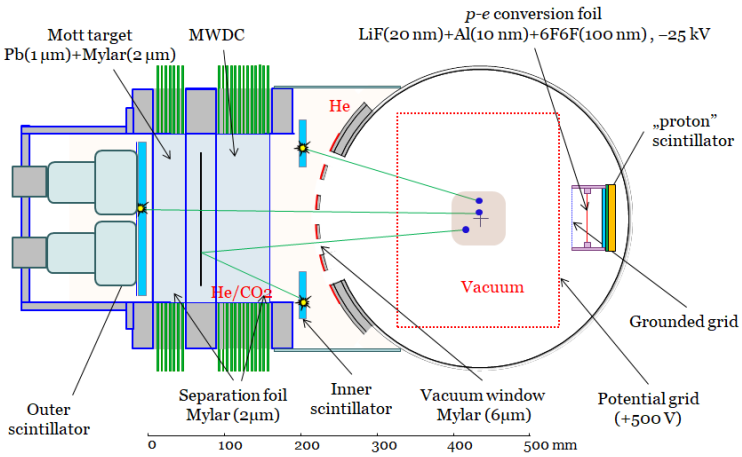

Figure 2. (Color on-line) Layout of the test experiment BRAND-0: Cross section in the plane perpendicular to the beam axis.

The cold neutron beam was transported along axis of a cylindrical vacuum chamber. A fraction of electrons from the neutron decay could leave the decay chamber through the thin side windows ($\approx$10 μm thick aluminized Mylar) and were registered in the electron detector consisting of tracking and plastic scintillator parts. Electron tracks were measured in e low density helium based (He:CO_2/85:15 + trace of ethanol vapor)[1] gaseous detector operated at ambient pressure. It was built as an 8 layer drift chamber of hexagonal cells. The track position in XY-plane was extracted from the measured drift time of ionization electrons whereas the position along the wire length (YZ-plane) was obtained by means of the charge division technique. The prototype electron tracker is a copy of the miniBETA spectrometer [22, 23]. Its properties are optimized for the energy range of electrons emitted in β-decays.

Electron tracking capability, a thin lead scatterer and additional scintillators at backward angles made this system an electron spin analyzer utilizing the Mott scattering. The Mott target (2 μm of Pb evaporated on 4 μm thick Mylar foil) was installed inside the tracker. Electrons passing the tracker and back-scattered by means of Mott process could be identified by characteristic track topology (called V-track). The energy of scattered electrons was measured in two, rectangular 10 mm thick plastic scintillators symmetrically positioned near to the tracker entrance window. The electrons transmitted through the Mott foil without significant scattering were registered in a circular 10 mm thick plastic scintillator installed behind the tracker. All scintillator detectors triggered DAQ, measured energy of registered electrons and provided the start signal for drift time measurement.

In the BRAND-0 setup, the proton detector prototype together with preamplifier boards was installed inside the decay chamber. Heat removal was accomplished with an ordinary cooling circuit. Stable temperature of about 12 ^{o}C was provided during measurements. Laboratory tests delivered the hit position resolution of such a system better than 3 mm [24].

[1]Less efficient but non-flammable gas mixture was used in the test due to safety regulations at ILL.

3.2 Analysis of test data

Accurate identification and precise tracking of electrons is crucial in the BRAND experiment since the transverse electron polarization is deduced from angular distribution in the Mott scattering. In the preliminary analysis of the collected data the average spacial resolution of MWDC in XY-projection deduced from drift time is about 0.4 mm (Fig. 3a) while the charge division technique provides 5 mm resolution in Z direction (Fig. 3b). An example V-track event topology is presented in Fig. 3c while the distribution of the reconstructed V-track vertex position is shown in Fig. 3d. A pronounced peak seen in this distribution at $X = 372$ mm points to the position of the Mott target. The scattering vertices in the Mott target are well separated from background ones attributed mainly to scattering on wires.

The obtained vertex position resolution of about 24 mm agrees with expectation. It should be pointed out that the prototype electron tracker fulfils the requirements posed by the BRAND project. The single cell position resolution deduced from drift time translates to the uncertainty of reconstructed angles in XY-projection. These, in turn, translate to the Mott scattering vertex position resolution critical for selection of events that belong to the Mott target. It is expected that the single cell position resolution should not exceed 0.7 mm. The vertex position resolution achieved in the test is roughly a factor of two worse than the required one. The difference with the expectation can be explained by the range of scattering angles accessible in the test that preferred acute V-track angles ($20^o - 40^o$). In the ultimate detector geometry, the V-track angles will range between $50^o - 80^o$.

The required Z-position resolution in the ultimate setup is estimated to about 25 mm. Taking into account wire length (reduced by a factor of five as compared to the ultimate solution), the resolution of 5 mm achieved in the test fulfills exactly the requirement.

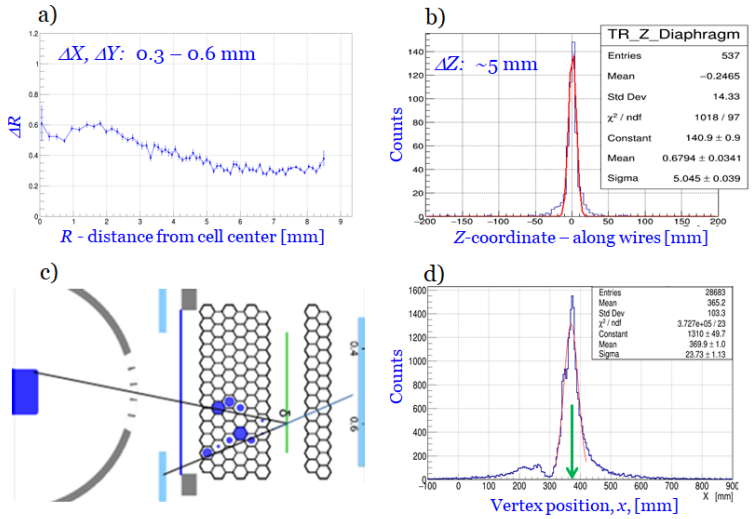

Figure 3. (Color on-line) Preliminary results achieved with the test setup BRAND-0. a) Position resolution extracted from drift time. b) Position resolution extracted from charge division technique. c) V-track event topology. d) Distribution of the reconstructed V-track vertex position (see text for more details).

The very short beam time available to the test and incomplete functionality of the trigger board and SiPM control system allowed only for initial performance test of the first prototype

proton detector. Equipped with a single 2 inch diameter circular converter foil the detector was tested in the self-triggering mode. The electric field configuration was optimized using COMSOL simulations. The goal was to collect as many as possible recoil protons emitted in the beam in order to increase the detection rate in a small detector (Fig. 4, left panel). In addition, the completed ad hoc high voltage system could sustain only about 16 kV so that the detector transmission was far from optimum. Nevertheless, we observed sensible behavior of rates and pulse height distribution. The plotted pulse height spectra reveal growing excess of counts and larger pulse height with increasing acceleration potential as shown in Fig. 4, right panel. Therein the line corresponding to −6 kV can be interpreted as the noise contribution. At this voltage the multiplicity of secondary electrons is significantly reduced [21] and the signal is obviously below the discrimination threshold. The increasing cage potential leads to increase of the proton acceleration potential and, consequently, to higher multiplicity of secondary electrons and larger signals as seen from Fig. 4, lower-right panel.

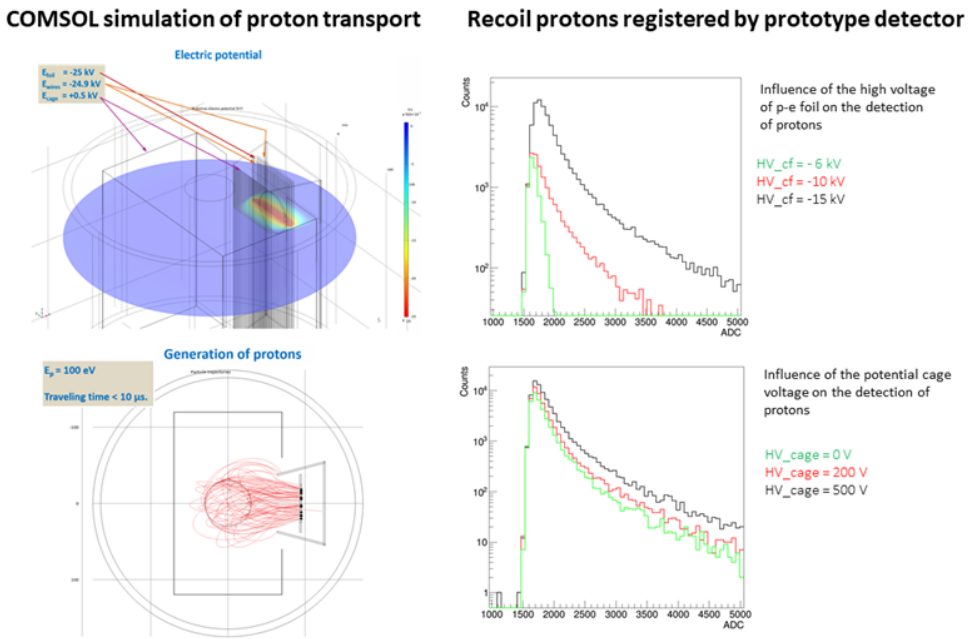

Figure 4. (Color on-line) Proton detector prototype in the self-triggering mode. Left panel: COMSOL simulation of proton transport. Right panel: Growing excess of counts with increasing acceleration potential.

Contrary to positive test results for the electron tracking and Mott polarimetry, it is clear that the proton detector prototype must be further improved. Among others the SiPM control and the gain calibration system (using alpha source) must be implemented before the hit position reconstruction will be possible.

4 BRAND-1 setup

Encouraging results from the first on-beam test of the detector prototypes led to the second experiment with improved components and the setup geometry closer to that of the ultimate experiment. Therein the Mott detectors are embedded in the MWDC. One of the important

goals for measurements with the BRAND-1 setup is to produce data with the complete chain of detectors, front end electronics and DAQ. Moreover, the neutron spin guiding field and periodic spin flip procedure is also implemented such that a full analysis of data and extraction of the correlation coefficients will be possible. Fig. 5 shows a sketch of the BRAND-1 setup. The apparatus was installed on the PF1B beam line at ILL, Grenoble and collected data within a four week long run starting in September 2021. Presently, the collected data are subject of intensive analysis.

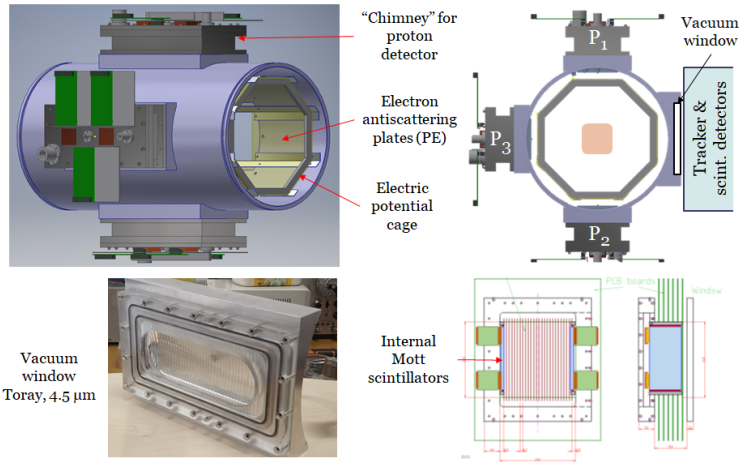

Figure 5. (Color on-line) BRAND-1 setup. Upper panel: Decay chamber with compartments for three proton detectors. Lower-left panel: Kevlar thread reinforced vacuum window prototype. Lower-right panel: Sketch of Mott detectors embedded in the electron tracker.

Acknowledgments: This work has been supported by the National Science Center, Poland, under the grant No. UMO-2018/29/B/ST2/02505. NCSU co-authors acknowledge the supporting grants from NSF: PHY-1914133 and DOE: DE-FG02-ER41042.

References

[1] A.N. Ivanov et al., Phys. Rev. C 95, 055502 (2017) and references therein.
[2] A.N. Ivanov et al., Phys. Rev. C 98, 035503 (2018) and references therein.
[3] J. Jackson et al., Phys. Rev. 106, 517 (1957).
[4] J. Jackson et al., Nucl. Phys. 4, 206 (1957).
[5] M.E. Ebel et al., Nucl. Phys. 4, 213, (1957).
[6] P.A. Zyla et al. (Particle Data Group), Prog. Theor. Exp. Phys. 2020, 083C01 (2020) and 2021 update.
[7] K. Bodek et al., EPJ Web of Conf. 219, 04001 (2019).
[8] V. Khachatryan, et al. CERN Rep. CMS-PAS-EXO-12-060, (2013).
[9] A. Kozela et al., Phys. Rev. Lett. 102, 172301 (2009).
[10] G. Ban et al., Nucl. Instrum. Methods Phys. Res., Sect. A 565, 711 (2006).
[11] K. Bodek et al., Physics Procedia 17, 30 (2011).
[12] A. Kozela et al., Phys. Rev. C 85, 045501 (2012).
[13] W. S. Wilburn et al., J. Res. NIST 110, 389 (2005).

[14] B. Maerkisch et al., Nucl. Instr. Meth. Phys. Res. A 611, 216 (2009).
[15] D. Dubbers et al., Nucl. Instr. Meth. Phys. Res. A 596, 238 (2008).
[16] O. Zimmer et al., Nucl. Instr. Meth. Phys. Res. A 440, 548 (2000).
[17] F.E. Wietfeldt et al., Nucl. Instr. Meth. Phys. Res. A 611, 207 (2009).
[18] B. Tipton et al., AIP Conf. Proc. 539, 286 (2000).
[19] R. Alarcon et al., URL http://nab.phys.virginia.edu/ nab_loi.pdf, Letter of intent (2005)
[20] H.P. Mumm et al., Rev. Sci. Instr. 75, 5343 (2004).
[21] S. Hoedl et al., J. Appl. Phys. 99, 084904 (2006).
[22] M. Perkowski et al., Acta Phys. Pol. 49 (2018), p. 261.
[23] M. Perkowski. PhD Thesis, Jagiellonian University and KUL, Krakow/Leuven, 2020.
[24] M. Kolodziej, Master Thesis, Jagiellonian University, Krakow, 2020.